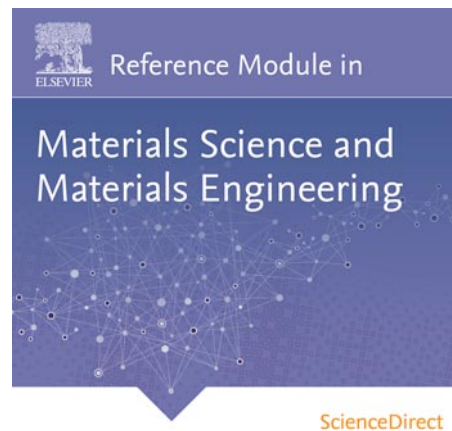


**Provided for non-commercial research and educational use.
Not for reproduction, distribution or commercial use.**

This article was originally published in the *Reference Module in Materials Science and Materials Engineering*, published by Elsevier, and the attached copy is provided by Elsevier for the author's benefit and for the benefit of the author's institution, for non-commercial research and educational use including without limitation use in instruction at your institution, sending it to specific colleagues who you know, and providing a copy to your institution's administrator.



All other uses, reproduction and distribution, including without limitation commercial reprints, selling or licensing copies or access, or posting on open internet sites, your personal or institution's website or repository, are prohibited. For exceptions, permission may be sought for such use through Elsevier's permissions site at:

<http://www.elsevier.com/locate/permissionusematerial>

Reshak A.H., Metal Hydrides: Electronic Band Structure. In: Saleem Hashmi (editor-in-chief), Reference Module in Materials Science and Materials Engineering. Oxford: Elsevier; 2017. pp. 1-16.

ISBN: 978-0-12-803581-8

Copyright © 2017 Elsevier Inc. unless otherwise stated. All rights reserved.

Metal Hydrides: Electronic Band Structure[☆]

AH Reshak, University of West Bohemia, Pilsen, Czech Republic and University Malaysia Perlis, Kangar, Malaysia

© 2017 Elsevier Inc. All rights reserved.

1	Methodologies	4
2	Binary Transition Metal Hydrides	5
3	Hydrides of Intermetallic Compounds	6
3.1	Hydrides of AB Compounds	6
	(a) Hydrides of ZrNi and ZrCo	6
	(b) Hydrides of FeTi and NiTi	7
3.2	Hydrides of AB ₅ (Hauke) Compounds	8
	(a) LaNi ₅ -H ₂ systems	8
	(b) Effects of substitutions	9
3.3	Hydrides of AB ₂ Laves Phases Compounds	10
	(a) Superconducting Laves phases	10
	(b) Hydrides of magnetic Laves phases	11
4	Hydrides of Intermetallic Compounds With Transition and Alkali or Alkaline-Earth Elements	12
4.1	Hydrides of the RNi ₃ - and R ₂ Ni ₇ -based (R=Light Rare Earth Element)	12
4.2	Mg ₂ NiH ₄ , Mg ₂ CoH ₅ , Mg ₂ FeH ₆ and Related Hydrides	12
4.3	Palladium-Based Ternary Hydrides	12
5	Perspective	13
	Acknowledgments	13
	References	13
	Further Reading	16

Metal hydrides represent promising technology for cleaner, cheaper and more efficient energy production [1–14]. They are also systems of considerable theoretical interest [15–25] convenient for investigation of fundamental interactions that are expected to be important in new complex materials [26–32]. Although significant experimental and theoretical work has been devoted to the study of metal hydrides, some of their fundamental features, such as details of valence and conduction bands and energy gap structures, the charge transfer and the charge distribution, the origin and the importance of various contributions to the bonding between metal and hydrogen (M–H) and hydrogen and hydrogen (H–H), are not yet fully clarified. A complete elaboration of these topics from the first principles is indispensable for understanding of H-behavior in metallic systems in general. Moreover, extensive data about metal hydrides have been obtained and explained using various, and sometimes contradictory, concepts [15–18,20–26,33–38]. However, a coherent approach valid for all metal hydrides is still missing. To better illustrate these points, attention will be focussed on one of the most investigated M–H systems, MgH₂, and extend the elaboration with some instructive and interesting examples found for other metal hydrides. Reshak [39] have performed a comprehensive theoretical investigation of the electronic band structure, density of states, electronic charge density and optical properties of the novel hydrogen storage material MgH₂ and LiH compounds. The all electron full potential linear augmented plane wave method was employed. The local density approximation (LDA), the generalized gradient approximation (GGA) and the Engle Vosko generalize gradient approximation (EVGGA) were used to treat the exchange-correlation potential. From the partial density of states and the electronic charge density in (0 0 1) and (1 0 1) crystallographic planes it has been found that there exists strong ionic bonds, see Fig. 1. The bond lengths were calculated and compared with the available experimental and theoretical results, the results show better agreement with the experimental values than the other theoretical results. The frequency dependent dielectric function's dispersions were calculated and analyzed so as to obtain further insight into the electronic structure.

Ivanović *et al.* [40] have presented approach to various metal hydrides based on electronic principles. The effective medium theory (EMT) was used to illustrate fundamental aspects of metal–hydrogen interaction and clarify the most important processes taking place during the interaction. The elaboration is extended using the numerous existing results of experiment and calculations, as well as using some new material. In particular, the absorption/desorption of H in the Mg/MgH₂ system is analyzed in detail, and all relevant initial structures and processes explained. Reasons for the high stability and slow sorption in this system are noted, and possible solutions proposed. The role of the transition–metal impurities in MgH₂ was discussed, and some interesting phenomena, observed in complex intermetallic compounds, were mentioned. The principal mechanism governing the Li-amide/imide transformation was also discussed. Latterly, some perspectives for the metal-hydrides investigation from the electronic point of view were elucidated.

[☆]Change History: July 2015. A.H. Reshak updated the whole of the article including many new references.

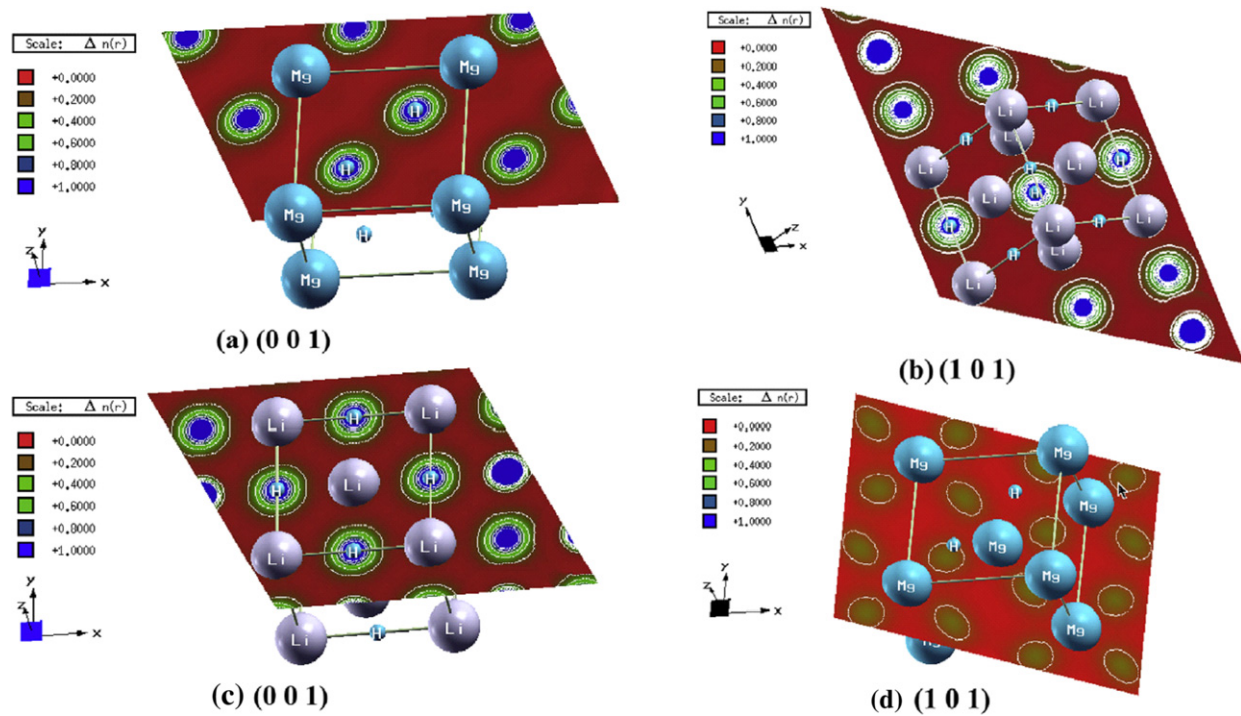


Fig. 1 Electronic charge density for (a) MgH_2 , (b) LiH , (c) LiH , and (d) MgH_2 .

Reshak *et al.* [41] reported a first-principles study of structural and phase stability in three different structures of perovskite-type KMgH_3 according to H position (Fig. 2). While electronic and optical properties were measured only for stable perovskite-type KMgH_3 (Fig. 3), the calculated structural parameters were found in good agreement with experiment and other theoretical results (see Table 1). The electronic charge density space distribution contours, which gives better insight picture of chemical bonding between K–H, K–Mg–H, and Mg–H, in the (2 0 0), (1 0 1), and (1 0 0) crystallographic planes were investigated. Moreover, the electronic band structure dispersion, total, and partial density of electron states were investigated to study the band gap origin and the contribution of s-band of H, s and p-band of Mg in the valence band, and d-band of K in the conduction band. Furthermore, optical features such as dielectric functions, refractive indices, extinction coefficient, optical reflectivity, absorption coefficients, optical conductivities, and loss functions of stable KMgH_3 were calculated for photon energies up to 40 eV.

In recent years, one can observe an enhanced interest to groups I–III of the periodic table, for example, K, Li, Na, Mg, Ba, Sr, and Al, to form different types of complex hydrides that are interesting for the use as potential hydrogen storage materials because of their light weight. Today a lot of research activity is in progress with the aim to identify new materials with high hydrogen content and suitability to functionalize at low operating temperature. Perovskite hydrides ABH_3 are gaining much interest because of cubic structure and presence of lightweight elements like CsCaH_3 , RbCaH_3 , KMgH_3 , BaLiH_3 , and SrLiH_3 . 1–4 Mg-based phases receive particular attention because of lightweight and low cost production. Recently, a number of theoretical studies were carried out for structural and electronic properties in different phases of MMgH_3 ($M = \text{Li, Na, K, Rb, Cs}$) [46,47]. For hydrides, owing to the complexity in structural arrangements and difficulties involved in establishing hydrogen positions by X-ray diffraction methods, structural information is limited [48]. However, most of these materials are not well-described and thermodynamic data are absent [49]. Some of theoretical results are available only for the stability of these perovskite hydrides XLiH_3 ($X = \text{Ba and Sr}$) [50] and XCaH_3 ($X = \text{Cs and Rb}$) [51] under pressure. But for Mg-based perovskite hydride KMgH_3 , no experimental or theoretical data for phase stability related to hydrogen positions are available. Keeping these points in view, we focus on stability of perovskite-type KMgH_3 according to different hydrogen positions and investigate the electronic and optical properties in that stable phase only.

Metal–hydrogen systems have been continuously investigated ever since the ability of metallic palladium to absorb large amounts of hydrogen was discovered in 1866. Besides the importance of these systems in fundamental solid-state and materials science, the concern for energy and environmental problems has provided further motivation for studying hydrogen in intermetallic compounds such as LaNi_5 since the discovery of the exceptional hydriding properties of this intermetallic by van Vucht *et al.* [52]. Several aspects of the research on metal–hydrogen systems can be found in reviews and books by Mueller *et al.* [53], Alefeld and Völkl [54], Buschow *et al.* [55], Schlapbach [56,57], Fukai [58], and Wipf [59].

The insertion of hydrogen in metallic matrices leads to drastic changes in their electronic structure, due in part to structural effects (volume change often accompanied by crystal structure modifications), but mainly due to chemical effects. The presence of hydrogen perturbs the metal–metal bonds and creates new metal–hydrogen interactions, and the additional electrons of the hydrogen atoms modify the electron count and the electronic properties at the Fermi level. For good hydrogen absorbers, the

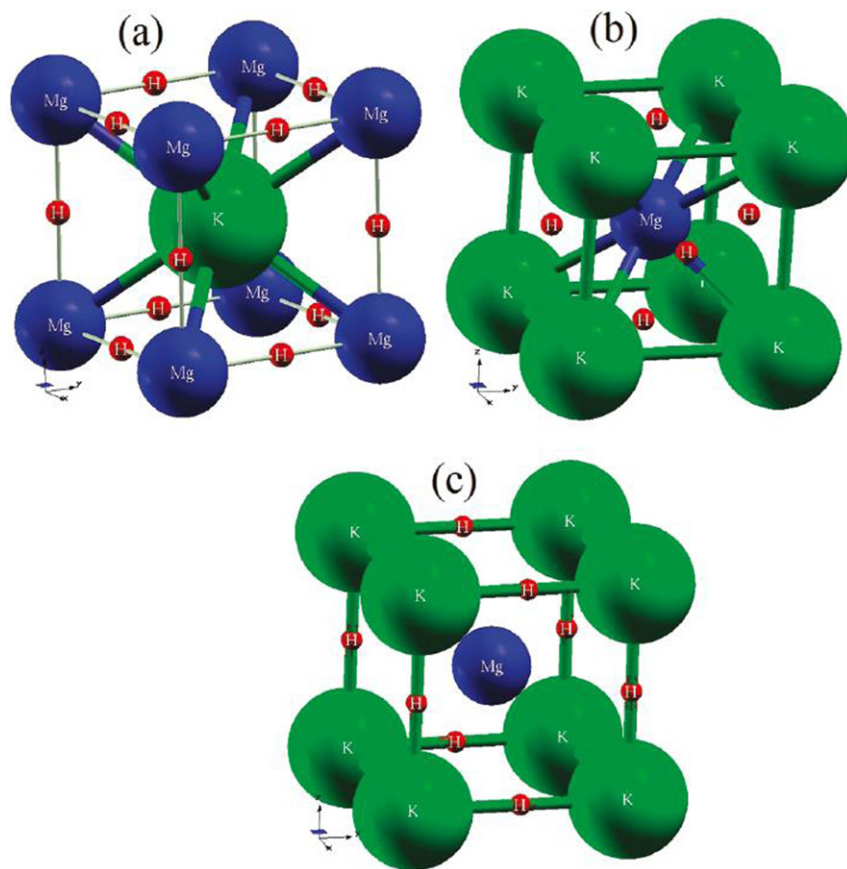


Fig. 2 Crystal structures of KMgH_3 (a) Stable, (b) US1, and (c) US2.

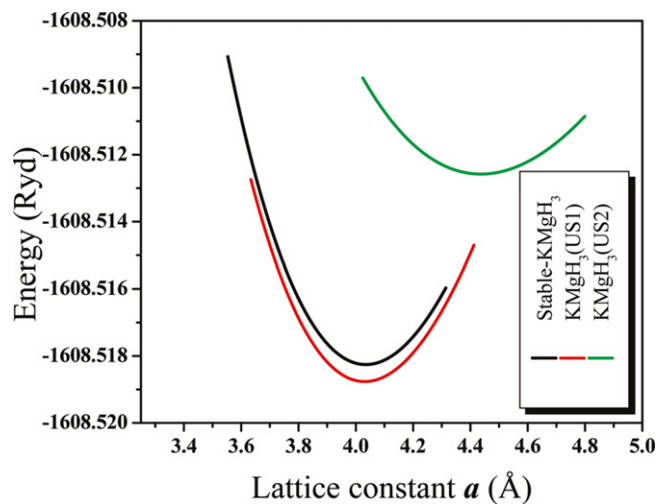


Fig. 3 Comparison of total energy vs. lattice constants for different phases of KMgH_3 with PBE-GGA approximation.

hydrogen per metal atom ratio can vary in a wide range of nonstoichiometry from the solid solution limit to concentrated hydride phases, and the electronic properties at the Fermi level can thus be tuned in a continuous and fascinating way. Electronic band structure studies are useful in understanding, at a microscopic level, the changes in the important physical properties of the matrices on hydrogen uptake such as metal–semiconductor transitions, magnetism, and superconductivity, and thermodynamic properties such as stability, maximum hydrogen absorption capacity, and preferential H site occupancy. A review of the present status, achievements, and limits of the electronic band structure studies of binary transition and rare earth metal hydrides as well as

Table 1 Atomic coordinates (K, Mg, H) calculated lattice constants a (Å), Bulk Modulus B_0 (GPa), derivative of bulk modulus B'_0 , elastic constants (GPa), nearest neighbor bond length distances (Å), and indirect band gap E_g (eV) for US1, US2, and stable phase of KMgH_3 compared with available other theoretical and experimental results

KMgH_3	US1	US2	Stable	Other theoretical	Experiment
Atomic coordinates					
K	(0 0 0)	(0 0 0)	(0.5 0.5 0.5)	(0 0 0) ^{b,c}	(0 0 0) ^d
Mg	(0.5 0.5 0.5)	(0.5 0.5 0.5)	(0 0 0)	(0.5 0.5 0.5) ^{b,c}	(0.5 0.5 0.5) ^d
H	(0.5 0.5 0)	(0.5 0 0)	(0 0 0)	(0.5 0.5 0.5) ^{b,c}	(0.5 0.5 0.5) ^d
a	4.034	4.44	4.035	4.0295 ^b , 4.01 ^c	4.023 ^a , 4.025 ^d
B_0	34.805	21.08	35.1008	35.6 ^b	
B'_0	3.77	4.19	3.57	3.7 ^b	
C_{11}	55.073	46.189	75.076		
C_{12}	8.684	19.723	19.752		
C_{44}	-24.438	-18.899	34.733		
nn Bond length distances					
K-H	2.85	2.219	2.853	2.85 ^b	
K-Mg	3.49	3.843	3.495	3.49 ^b	
Mg-H	2.02	3.138	2.018		
H-H	2.85	3.138	2.853		
$E_g(\text{X-R})$	2.23		2.53	2.32 ^b , 2.6 ^e	

^aRef. [42].

^bRef. [43].

^cRef. [44].

^dRef. [45].

^eRef. [46].

of complex intermetallic hydrides follows, with a particular emphasis on compounds of potential importance for technological applications.

1 Methodologies

The electronic structure problem for a solid involves the study of the light particles, the electrons which, in the Born–Oppenheimer approximation, are assumed to be moving in the electrostatic field of the fixed heavier particles, the nuclei. The energy of the electronic ground state obtained as a function of the fixed nuclei can then be used as a potential energy for the motion of the nuclei. Since the Schrodinger equation of a system of N interacting particles cannot be solved exactly, it is usually replaced by an effective Schrodinger equation for one electron moving in the mean field of the other electrons and nuclei. The mean field used for solids is often based on the local density approximation (LDA) of the density functional theory (DFT) developed in the mid-1960s by Hohenberg and Kohn [60]. Besides the electrostatic interactions with the nuclei, this mean field is composed of the Coulomb repulsion due to the electron charge cloud and the exchange and correlation terms; it depends only on the electron density, $\rho(r)$. In the LDA, the exchange and correlation term is obtained from the many-body theory applied to the electron gas having local density $\rho(r)$. The different ab initio techniques used in band structure calculations depend essentially on the approximations used for calculating the effective potential, and on the nature of the basic functions that can be fixed (plane waves, linear combination of atomic orbitals) or energy and potential dependent, as in the augmented plane waves (APW) method. The linear methods such as the linear muffin-tin orbital method (LMTO) and LAPW, use energy-independent basis functions derived from partial waves and combine the advantages of the two methods (see Refs. [61] and [62] for reviews); they allow systems of complex structures to be studied using either approximate or full potential treatment. From these studies, total energies, lattice parameters, elastic properties, and even fully relaxed structures can, in principle, be obtained. Using the spin-polarization techniques with spin-dependent electron densities, magnetic systems can also be studied. Improvements beyond the LDA can be included using, for example, the generalized gradient approximation (GGA). In calculating the self-consistent band structure within DFT, both LDA and GGA usually underestimate the energy gap [63]. This is mainly due to the fact that they have simple forms that are not sufficiently flexible to accurately reproduce both the exchange–correlation energy and its charge derivative. Engel and Vosko [64] considered this shortcoming and constructed a new functional form of GGA that is able to better reproduce the exchange potential at the expense of less agreement in the exchange energy. This approach, called EV-GGA, yields better band splitting and some other properties that mainly depend on the accuracy of the exchange–correlation potential. On the other hand, the quantities that depend on an accurate description of Ex, such as the equilibrium volume and bulk modulus, are in poor agreement with experiment [63,65]. To overcome this drawback, Tran and Blaha [66] have proposed a new approach called mBJ. The mBJ, a modified Becke–Johnson potential, allows the calculation of band gaps with accuracy similar to the very expensive GW calculations [66]. It is a local approximation to an atomic “exact-exchange” potential and a screening term. The GW approximation can partly

correct the correlation effects, where G is the exact one-particle Green's function and W the screened Coulomb interaction, GW calculation is time demand and CPUs consuming.

In the recent years due to the improvement of the computational technologies, it has been proven that the first-principles calculation is a strong and useful tool to predict the crystal structure and its properties related to the electron configuration of a material before its synthesis.

2 Binary Transition Metal Hydrides

Metal hydrides with enhanced thermodynamic stability with respect to the associated binary hydrides are useful for high temperature applications in which highly stable materials with low hydrogen overpressures are desired. Though several examples of complex transition metal hydrides (CTMHs) with such enhanced stability are known, little thermodynamic or phase stability information is available for this materials class. In this work, we use semiautomated thermodynamic and phase diagram calculations based on DFT and grand canonical linear programming (GCLP) methods to screen 102 ternary and quaternary CTMHs and 26 ternary saline hydrides in a library of over 260 metals, intermetallics, binary, and higher hydrides to identify materials that release hydrogen at higher temperatures than the associated binary hydrides and at elevated temperatures, $T > 1000\text{K}$, for 1 bar H_2 overpressure. For computational efficiency, we employ a tiered screening approach based first on solid phase ground state energies with temperature effects controlled via H_2 gas alone and second on the inclusion of phonon calculations that correct solid phase free energies for temperature-dependent vibrational contributions. We successfully identified 13 candidate CTMHs including Eu_2RuH_6 , Yb_2RuH_6 , Ca_2RuH_6 , Ca_2OsH_6 , Ba_2RuH_6 , $\text{Ba}_3\text{Ir}_2\text{H}_{12}$, Li_4RhH_4 , NaPd_3H_2 , Cs_2PtH_4 , K_2PtH_4 , Cs_3PtH_5 , Cs_3PdH_3 , and Rb_2PtH_4 . The most stable CTMHs tend to crystallize in the Sr_2RuH_6 cubic prototype structure and decompose to the pure elements and hydrogen rather than to intermetallic phases (see Ref. [67]).

In most of the stable metal hydrides, a simple interpretation of the band structure can be obtained in the following way: since the hydrogen potential is more attractive than the metal atom potential, the lowest energy bands result from the hydrogen–metal bonding and H–H antibonding interactions. The number of corresponding bands is usually equal to the number of hydrogen atoms in the unit cell. The extent of the overlap of these states with higher energy metal states depends on a number of factors such as the energy difference between the metal and H orbitals, and the H–H distances; short H–H distances lead to an increase of the overlap due to a destabilization of the H–H antibonding states usually located at the top of the low-energy H-derived bands. The Fermi level position of the hydride depends crucially on the imbalance between the number of hydrogen-induced new states created below the Fermi level of the pure metal and the number of additional electrons per unit cell brought by the hydrogen atoms. This can either lead to a filling of the metal d bands as in the monohydrides, PdH and NiH, or to a depopulation of the pure metal d states in the early transition metal and rare-earth di- and trihydrides. The electronic structure of rocksalt structure hydrides of transition metals of the end of the series such as palladium and nickel has been investigated since the early 1970s (see Refs. [68] and [69] for reviews). It has been shown in great detail that the filling of the metal d bands in the stoichiometric hydride, leads to a drastic decrease of the densities of states at the Fermi level and the disappearance of ferromagnetism in nickel and of spin fluctuations of pure palladium. The Fermi surfaces of the monohydrides are topologically similar to those of noble metals; however, the protonic rigid band model is not quantitatively correct. Band structure calculations have been helpful in evaluating the electronic part of the electron–phonon coupling constant l that controls the superconducting critical temperature T_c in normal superconductors. In PdH ($T_c=9\text{K}$), and its alloys with noble metals, it is the electron–optical phonon coupling that is responsible for the superconducting properties. The role played by the presence of hydrogen s states at the Fermi energy and the low frequencies of the optic modes has been stressed [70]. Although metal–insulator transitions occurring in bulk yttrium and rare-earth hydrides for hydrogen/metal ratios approaching 3 have been thoroughly investigated (see Ref. [71] for review), studies of the spectacular optical properties of switchable mirrors based on thin films of YH_x and LaH_x initiated by Huiberts *et al.* [72] have renewed the interest in the fundamental understanding of the metal–insulator transition as a function of x . The metallic properties of dihydrides of trivalent transition metal are very well accounted for by self-consistent band structure calculations. In the dihydrides, the five valence electrons occupy the two low-energy bands associated with metal–hydrogen and hydrogen–hydrogen bonding and the Fermi level falls at bottom of the metal d bands that accommodate the remaining electron. This feature of the electronic structure of early transition metal hydrides has been often interpreted in terms of a depopulation of the metal d bands in favor of the bonding low energy bands. In fact, in these hydrides the proton is better screened than in PdH or NiH.

In trihydrides of trivalent rare earth, since three M–H and H–H bands are formed below the pure metal d states, a semi-conducting or semimetallic behavior is expected for these 6 valence electron systems, depending on the existence of an energy separation or an overlap of the two manifolds. However, band structure calculations within the LDA [73] lead to a band overlap larger than 1 eV for YH_3 in the hexagonal HoD_3 structure and thus to a metallic state while an optical energy gap of about 2.8 eV is observed in reflection and transmission for YH_3 . Although LDA is known to underestimate band gaps in other types of semiconductors or insulators, the discrepancy obtained for YH_3 seems particularly large and led to further interpretations involving broken symmetry structures and many-body effects beyond the LDA. Using parametrized model hamiltonians, Eder *et al.* [74] showed that strong correlation effects associated with H^- ions can open a substantial gap due to an energy lowering of the H-valence bands; the singlet formed by the two electrons on the H^- ion bears some similarities with the Zhang–Rice singlet coupling two holes in the high- T_c cuprate superconductors. Electromigration experiments of van der Molen *et al.* [75] tend to be in support of this picture. Ng *et al.* [76] also found that many-body effects result in a gap due to a narrowing rather than to an energy

lowering of the H-derived bands. Other possible mechanisms such as symmetry-breaking distortions due to hydrogen displacements have been considered in particular by Kelly *et al.* [77] on the basis of minimum energy structures. Although such symmetry breaking can lead to large gaps, these predictions have not been so far confirmed by the neutron diffraction experiments of Udovic *et al.* [78].

The relevance of the comparison of gaps obtained from band structure calculations that probe only ground state properties and optical gaps that probe symmetry-allowed direct transitions has been questioned by van Gelderen *et al.* [79]. Parameter-free quasiparticle calculations in the GW approximation lead to a gap of 1 eV while inclusion of the electric dipole matrix elements give a larger optical gap of about 3 eV. According to another GW calculation by Miyake *et al.* [80], the existence of a gap is due to many-body effects, and does not depend on the exact crystal structure; however, the gap is not due to a narrowing of the H-derived bands but rather to an upward shift of the unoccupied yttrium 4d states. Ab initio calculations of the lattice dynamics of YH₃ in the HoD₃ and in symmetry-broken structures by van Gelderen *et al.* [81], compared with the high-resolution neutron vibrational spectroscopy data of Udovic *et al.* [78] support the existence of symmetry lowering in YH₃.

Thus, in spite of the most recent developments using state-of-the-art calculations, and experimental data such as neutron scattering and NMR electric field gradient [82], the most stable crystal structure and the origin and value of the energy gap of YH₃ are still a matter of debate. For h.c.p. yttrium, the hydrogen solid solution region has been investigated by Wang and Chou [83] by total energy calculations using pseudopotentials (PP) and plane-wave (PW) basis within the LDA. From their total energy calculations, they found that the tetrahedral sites are more stable than the octahedral ones. A study of various pairings of the hydrogen atoms shows, in agreement with experimental data, that the linear ordering of pairs at the tetrahedral sites bridged by a metal atom is favored.

3 Hydrides of Intermetallic Compounds

Interaction of intermetallic compounds with ammonia was studied as a processing route to synthesize hydrides and hydridonitrides of intermetallic compounds having various stoichiometries and types of crystal structures, including A₂B, AB, AB₂, AB₃ and A₂B₁₇ (A=Mg, Ti, Zr, Sc, Nd, Sm; B=transition metals, including Fe, Co, Ni, Ti and nontransition elements, Al and B). In presence of NH₄Cl used as an activator of the reaction between ammonia and intermetallic alloys, their interaction proceeds at rather mild *P-T* conditions, at temperatures 100–200°C and at pressures of 0.6–0.8 MPa. The mechanism of interaction of the alloys with ammonia appears to be temperature-dependent and, following a rise of the interaction temperature, it leads to the formation of interstitial hydrides; interstitial hydridonitrides; disproportionation products (binary hydride; new intermetallic hydrides and binary nitrides) or new metal–nitrogen–hydrogen compounds like magnesium amide Mg(NH₂)₂. The interaction results in the synthesis of the nanopowders where hydrogen and nitrogen atoms become incorporated into the crystal lattices of the intermetallic alloys. The nitrogenated materials have the smallest particle size, down to 40 nm, and a specific surface area close to 20 m² g⁻¹ (see Ref. [84] for reviews).

ZrNi was the first intermetallic compound found to reversibly absorb hydrogen [85], thus opening a new field of investigation. A large amount of experimental research on LaNi₅ and related compounds was initiated by the work of van Vucht *et al.* [52]. The development of applications of intermetallics, in particular for energy storage (see Ref. [86] for a review), led to the search for new hydrogen-absorbing materials. The hydriding properties of AB-type compounds such as FeTi found by Reilly *et al.* [87] as well as other intermetallic compounds such as Laves phases AB₂ have been thoroughly investigated. Band structure studies started only in 1982 (see Ref. [69] for review of the early work). An increasing number of ab initio investigations of these complex structure systems have become available since then. However, theoretical work on the fascinating role of hydrogen on the magnetic properties of intermetallic compounds (see Refs. [55] and [88] for reviews) remains to be developed.

3.1 Hydrides of AB Compounds

(a) Hydrides of ZrNi and ZrCo

Zirconium cobalt alloy is one of the strongest candidate materials for capturing and transferring hydrogen or hydrogen isotopes, especially tritium [89] as storage, supply and recovery in thermonuclear fusion devices. The hydride form of zirconium cobalt (ZrCo) is denoted by ZrCoH_x, where x is 1, 2 and 3 in general. It has been selected as reference material for the storage of hydrogen isotopes because of its good properties, which are comparable to those of uranium (ease activation, low equilibrium pressure of hydrogen at room temperature and moderate temperatures to release hydrogen gas), in particular with regard to a very low dissociation temperature leads to one bar hydrogen pressure. Important advantages of ZrCo over uranium are its non-nuclear character and its much lower pyrophorosity both in the metal and in the hydride form [90,91]. Because of this has been selected as a potentially substituted getter material for uranium by the International Thermonuclear Experimental reactors (ITER) team [92] (see Ref. [93] for review).

The maximum hydrogen absorption of ZrNi leads to the formation of ZrNiH₃ which crystallizes within the CrB-type orthorhombic structure, with a lattice expansion of about 20%. The total density of states (DOS) of the hydride, obtained by LMTO calculations [94] is plotted in Fig. 4. It is characterized as follows: (1) The presence of structure below -4 eV corresponds to metal–hydrogen bonding and H–H interactions. The energy position of this bonding structure agrees with photoemission and X-ray emission data. The contribution of the nickel 3d states to the metal–hydrogen bonding is sizeable although it is lower than

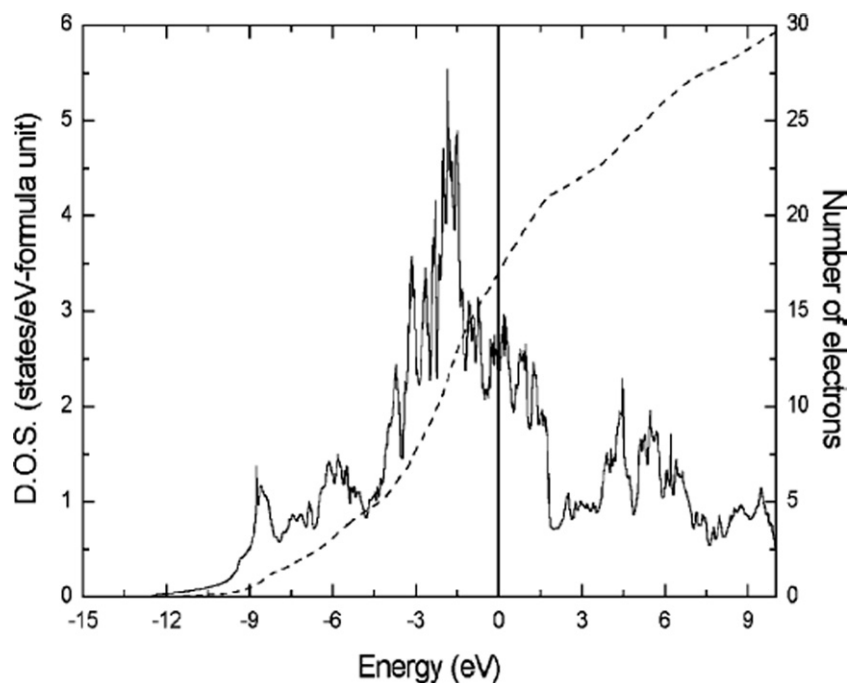


Fig. 4 Total density of states of ZrNiH_3 ; solid line, left-hand side scale; number of electrons, dashed line, right-hand side scale. The origin of energies is the Fermi energy.

that of the zirconium 4d states. This is due to the larger coordination number of hydrogen with zirconium in the pyramidal Zr_3Ni_2 and the tetrahedral Zr_3Ni sites. (2) The peak of the DOS centered around -3 eV is mostly due to nickel 3d states hybridized with zirconium 4d. (3) The main zirconium 4d structure with a weak admixture of nickel 3d character is located above the Fermi energy. The zirconium 4d DOS is considerably modified by the presence of hydrogen. The total DOS decreases slightly from ZrNi to ZrNiH_3 ; the zirconium d contribution at E_F decreases from 68% in the intermetallic to 62% in its hydride due to the broadening of the zirconium states and a slight lowering of E_F . This feature, which is important for the stability of the hydride, is due to the fact that the Zr-H interaction is strong enough to lower below E_F empty zirconium states of the pure intermetallic compound. In contrast, the Ni-H interaction stabilizes in energy nickel d states already occupied in ZrNi , and thus does not contribute to the lowering of E_F .

A very unusual feature of the ZrNi-H_2 system is that the Zr_4 (4c) sites that are occupied in triclinic ZrNiH become empty in favor of the pyramidal Zr_3Ni_2 (4c) and tetrahedral Zr_3Ni (8f) sites in ZrNiH_3 . Total energy calculations were performed for ZrNiH for two possible occupancies of H sites, Zr_4 (4c) and Zr_3Ni_2 (4c). Both sites satisfy the usual geometric criteria of minimum hole size and minimum H-H distances. In agreement with neutron scattering data of Westlake *et al.* [95], the chemical effect associated with the Zr-H interaction and the Fermi level position result in a greater stability of the Zr_4 sites. At higher hydrogen concentration, the repulsive H-H interaction at short distances leads to the site occupancy observed in ZrNiH_3 . ZrCo is also a good hydrogen absorber that has been considered since the late 1980s as a possible substitute for uranium for the storage of hydrogen and its radioactive isotope, tritium. ZrCoH_3 is isostructural to ZrNiH_3 . The main differences in the DOS of the two hydrides can be summarized as follows: the cobalt 3d structure is broader and located at higher energy than the nickel 3d peak, leading to a larger overlap with the zirconium 4d states. Since the electron count decreases by one per formula unit from ZrNiH_3 to ZrCoH_3 , the Fermi level is closer to the cobalt d peak and the total DOS of ZrCoH_3 is 30% larger than that of the CsCl structure ZrCo . This indicates a tendency toward magnetic ordering. In ZrCoH_3 the metal-hydrogen bonding states are centered around 7 eV below E_F , in agreement with photoemission data reported by Gupta and Schlappbach [69].

(b) Hydrides of FeTi and NiTi

In particular, Ti-based binary intermetallic compounds (FeTi, CoTi and NiTi) have many interesting properties such as high hardness, high melting temperature, shape-memory effect, the high hydrogen capacity per unit weight [96], etc. Thus, they are very promising and potential candidates as future hydrogen storage materials (HSM) thereby they have received considerable attention. FeTi was studied as a potential candidate for on-board applications, due to its inexpensive price, reversible character for hydriding/dehydriding at near ambient condition, relative good storage capacity of 1.9 wt% whereas showing a poor kinetics of H_2 absorption/desorption [97]. Reilly and Wiswall [98] have observed that, when H_2 interacts with FeTi intermetallic compound, two ternary hydrides are produced FeTiH and FeTiH₂. These hydrides may easily decompose (release of H_2) thereby are very useful as H_2 storage media.

FeTi is a Pauli paramagnet of cubic CsCl-type ordered structure. As in isoelectronic and isostructural b.c.c. chromium, the Fermi level falls in the valley of the DOS between occupied d -like bonding states derived primarily from iron and empty d -like antibonding states derived mostly from titanium. In β -FeTiH, hydrogen occupies distorted octahedral Fe_2Ti_4 sites instead of the more usual tetrahedral sites characteristic of the b.c.c. metals. β -FeTiH has an orthorhombic structure. The analysis of APW band structure calculations shows that the metal–hydrogen bonding states, centered at 9 eV below E_F , are mainly due to the Fe–H interaction that lowers states already filled in the intermetallic. The Ti–H contribution to the bonding is not as large in spite of the greater affinity of hydrogen for titanium; however, this interaction brings new states below E_F . The Fermi level of β -FeTiH is found at higher energy than in FeTi, above the valley of the DOS; the calculated DOS at E_F increases from the intermetallic to its hydride in agreement with the observed increase in the magnetic susceptibility and the electronic specific heat.

The electronic structure of FeTiH₂ has been studied ignoring the monoclinic distortion. The low energy bonding structure grows in width and intensity upon increasing the hydrogen content. The contribution of Ti–H bonding is much larger than in FeTiH since one of the four hydrogen atoms in the unit cell is located closer to two titanium atoms rather than to the iron atoms. The Fermi level of FeTiH₂ falls above the valley of the DOS; it is, however, closer to the iron peak than in FeTiH due to the presence of a second H–H derived band at low energies.

Mossbauer isomer shift (IS) experiments reveal a systematic decrease of the s contact electron density at the metal site with hydrogen uptake that cannot be explained by a simple renormalization of the wavefunctions due to lattice expansion. Theoretical calculations show that the depletion of the $4s$ metal states at the iron site is due mostly to the Fe–H bonding contribution.

In the hydride of the shape memory alloy NiTi, the bonding properties are similar to those discussed for FeTi. The hydrogen absorption leads also to an upward shift of the Fermi level and the nesting features of the Fermi surface of NiTi disappear. The premartensitic phase transition of NiTi that arises from the condensation of a soft phonon is believed to be due to strong electron–phonon coupling of nested electronic states at E_F . No martensitic transformation occurs in the hydride.

3.2 Hydrides of AB₅ (Haucke) Compounds

In Haucke AB₅ compounds as well as in most H-absorbing transition metals and intermetallic compounds (IMC), the hydrogen absorption is accompanied by a large volume increase, the compressibility of the matrix is expected to play an important role. The elastic energy spent in the lattice expansion and the energy gained from the chemical metal–hydrogen interaction are indeed the antagonist key factors that control the stability of the hydrides. While the latter is of pure electronic origin, the former involves electronic as well as lattice properties. Substitutions at the A or B sites by elements of different sizes and (or) chemical nature are expected to affect both the electronic and elastic properties of the IMCs and consequently their hydrogen absorption properties. Experimentally, substitutions have been widely used to modulate the thermodynamic properties of hydrogen absorbing IMCs, and modify two parameters crucial for the applications of these materials, namely the plateau pressure of the hydrogen desorption isotherms and the maximum hydrogen absorption capacity [56,57,99]. Empirical correlations have been established between the value of the plateau pressure of the isotherms, pH_2 , and (1) the unit cell volume [100,101] and (2) the compressibility of the lattice estimated from measurements of the Debye temperature [100,102,103]. These experimental results indicate that the plateau pressure of the isotherms, pH_2 , decreases with increasing unit cell volume of the IMC, and with increasing value of the compressibility. However, considering the approximations on which the estimates of the compressibility rely, these correlations need further investigations. In very recent years, an increasing number of measurements by ultrasonic techniques of the elastic properties of hydrogen absorbing Laves phase [104] as well as substituted Haucke compounds became available [105,106] while theoretical calculations remain very scarce [107] (see Ref. [108] for review).

(a) LaNi₅–H₂ systems

Several investigations of this system in the solid solution and concentrated hydride phases have been performed since the last review [69] using the LMTO [109], the tight binding LMTO [110], and plane wave pseudopotential (PWPP) methods within the GGA [111]. LaNi₅ crystallizes in the hexagonal CaCu₅ structure, space group P6/mmm, in which the lanthanum atoms occupy the (1a) sites; there are two types of nickel atoms occupying, respectively, the (2c) sites in the basal lanthanum planes ($z=0$), and the (3g) sites in the middle plane ($z=c/2$). The occupied part of the conduction band is dominated by the nickel 3d states with a non-negligible bonding contribution of lanthanum 5d states. The main part of the lanthanum 5d states is, however, located above the Fermi energy.

The 4f states are empty; they are very localized at energies 3 eV above E_F . The nickel d bands are not filled and the intermetallic is not a charge transfer compound as shown by core level photoemission spectroscopy, which does not indicate any significant shift in the lanthanum 3d and nickel 2p core states in LaNi₅. The calculated total DOS is in agreement with XPS data concerning the width of the occupied states and the high emission observed at E_F . The DOS at E_F is high and mostly composed of nickel d states since the lanthanum d contribution is only 4%. This result is in agreement with low-temperature heat capacity measurements which lead to large values of the electronic specific heat coefficient and with magnetic susceptibility data. In spite of the large value of the DOS, LaNi₅ is found experimentally to be a Pauli paramagnet, although spin polarized band structure calculations [110] lead to a magnetic moment of about 0.6 mB per formula unit. The crystal structure of LaNi₅H₇ has been repeatedly examined by neutron diffraction (see Ref. [112] for review). Although satisfactory refinements have been obtained in the P63mc and the P31c space groups, which differ by the presence of a mirror plane, total energy calculations of Tatsumi *et al.* [111] favor the P63mc structure by 0.34 eV per LaNi₅.

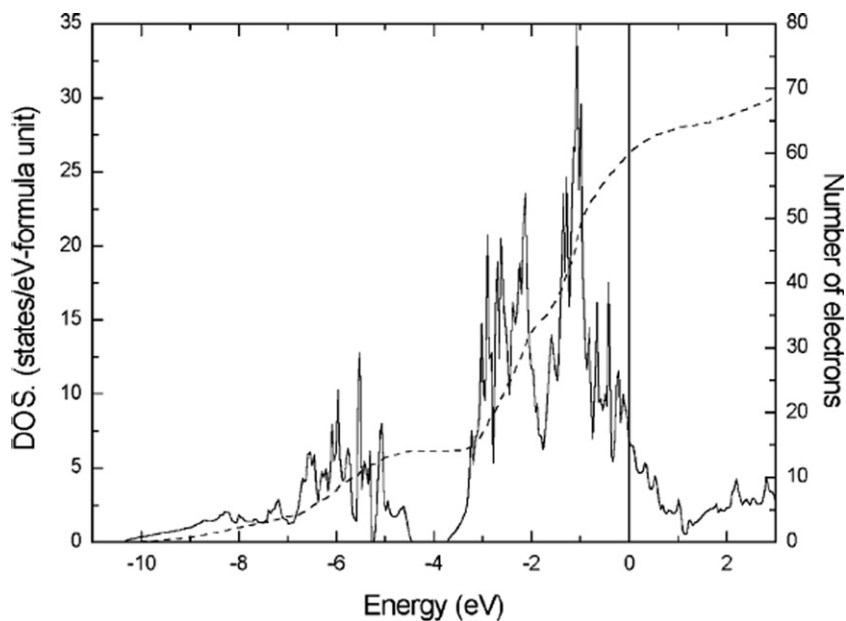


Fig. 5 Total density of states of LaNi_5H_7 : solid line, left-hand side scale; number of electrons, dashed line, right-hand side scale. The origin of energies is the Fermi energy.

The DOS of LaNi_5H_7 obtained by the LMTO method is shown in Fig. 5. The low-energy structure, extending down to 10 eV below EF, corresponds to seven bands associated with M–H and H–H interactions. The nickel contribution to the hydrogen bonding is larger than the lanthanum contribution. The nickel d states are not entirely filled in the hydride, and thus the DOS at EF remains large in the hydride although a decrease is found from its value in the intermetallic in agreement with the trends observed in electronic specific heat and magnetic susceptibility data.

In the solid solution LaNi-H within the $P6/mmm$ space group, five non-equivalent interstices have been proposed as possible H sites. The total energy calculations of Tatsumi *et al.* [111] for $\text{La}_2\text{Ni}_{10}\text{H}_1$ using the five possible H site occupancies and including geometry optimization indicate that the (12n) site appears to be the most energetically favorable, in agreement with neutron scattering data.

Experimental values of the heats of formation remain difficult to predict accurately from *ab initio* calculations since they result from the subtraction of very large values of total energies. Nevertheless, using full geometry optimization, Tatsumi *et al.* [111] obtained a heat of formation of $-33 \text{ kJ mol}^{-1} \text{ H}_2$ for the primary solid solution, in rough agreement with experimental data and a heat of formation of $-45 \text{ kJ mol}^{-1} \text{ H}_2$ for LaNi_5H_7 , a value that is 30–40% lower than the experimental one.

(b) Effects of substitutions

Substitutions at the lanthanum or nickel sites are used experimentally to modify the thermodynamic properties and play an important role in the selection of the alloys for specific technological applications, since they affect the stability and the maximum hydrogen content (for review see Refs. [113] and [112]). In order to optimize the choice of intermetallic compound, a better understanding of the role of each alloy constituent on the electronic properties of the material is crucial. Several semiempirical models (see Ref. [114] for review) have been proposed for the heat of formation and the heat of solution of metal hydrides and attempts have been made to justify the maximum hydrogen absorption capacity of the matrices. These models show that the energetics of the metal–hydrogen interaction depend both on geometric and electronic factors.

The effect of replacement of nickel by the 3d elements manganese, iron, or cobalt, by an s–p element of the 3d series such as copper, as well as by s–p elements such as aluminum and tin have been investigated by LMTO band structure calculations of ordered systems, thus ignoring the effect of disorder and the possible clustering of substituted elements. Neutron scattering data show that the nickel substitutions considered here occur predominantly at the nickel (3g) sites, in agreement with total energy calculations which indicate that substitutions at the nickel (3g) site are energetically preferred over nickel (2c) by several milli-Rydberg (mRy). Substitutions of nickel neighbors, M, on the left of the periodic table ($M = \text{Mn, Fe, Co}$) does not just lead to a simple depopulation of the nickel 3d bands. In all the substituted intermetallics a new narrow sub-band, associated with the 3d states of the substituting element M, appears slightly above the nickel d bands. The Fermi level of the substituted intermetallic falls in all cases in the narrow antibonding sub-band of the M element while the main nickel 3d structure is filled. As a consequence, the DOS at the Fermi level increases further from LaNi_5 to LaNi_4M ($M = \text{Mn, Fe, Co}$) indicating the possibility of magnetic ordering as found in spin-polarized calculations by Yang *et al.* [115]. In contrast, for $M = \text{Cu}$, the copper 3d sub-band is centered below the main nickel d peak in agreement with photoemission data. The substitution of nickel by copper or by an s, p element such as aluminum or tin leads to a decrease of the DOS at E_F associated with the progressive filling of the nickel d bands.

The heats of formation of the substituted alloys LaNi_4M ($\text{M}=\text{Mn, Fe, Co, Cu}$) have been measured by calorimetric methods. In all cases, the substituted intermetallics are less stable than LaNi_5 . Band structure calculations indicate that the effect of chemical substitution plays an important role in the observed decreased stability of LaNi_4M compared to LaNi_5 since the lattice expansion alone accounts for less than 50% of the decohesion of the alloy.

The electronic structures of some hydrides of substituted intermetallic compounds have been studied. In $\text{LaNi}_4\text{CoH}_4$, the Fermi level corresponds to a filling of the main cobalt 3d peak. The maximum hydrogen content appears to be associated with the filling of the cobalt d peak: further shift of the Fermi energy in the lanthanum 4d bands would cost energy since the DOS is not too high.

3.3 Hydrides of AB₂ Laves Phases Compounds

Amongst the intermetallic compounds, the Laves phases have been widely investigated in connection with their superconducting and magnetic properties (see Ref. [56] for review), but also as structural materials due to their high melting temperature and high strength, and as hydrogen storage materials. Besides the rich field of potential applications of the Laves phase hydrides, the understanding of the modifications of the electronic and magnetic properties on hydrogen absorption is of fundamental interest. Although electronic structure studies of many cubic (C-15) and hexagonal (C-14 and C-16) intermetallic compounds are available, band structure calculations of the corresponding hydrides remain rather scarce.

(a) Superconducting Laves phases

In the superconducting AB₂ Laves phases ($\text{A}=\text{Zr, Hf}$, $\text{B}=\text{V}$) with superconducting critical temperatures $T_c=8\text{K}$ for ZrV_2 and $T_c=9\text{K}$ for HfV_2 , the electron-phonon coupling is expected to be strongly affected by both the lattice expansion and by the change in the nature of the electronic states at E_F on hydrogen absorption.

ZrV_2 crystallizes within the C-15 cubic phase above $T_m=100\text{K}$; below this temperature it undergoes a rhombohedral distortion [116]. The interplay between structural and superconducting transitions also observed in the superconducting A-15 materials was widely discussed in the mid-1970s since they are both indicative of large electron-phonon coupling.

The total density of states of the cubic phase is plotted in Fig. 6. The Fermi energy falls in the transition metal (TM) d bonding bands close to a peak in the DOS. In agreement with previous work by Klein *et al.* [117], the value of the DOS at E_F is found to be large and dominated by the vanadium 3d contribution, which is about 50% larger than that of the zirconium 4d states. The large value of the DOS at E_F is consistent with the large magnetic susceptibility above T_m , as well as with the value of the electronic specific heat coefficient obtained from low temperature microcalorimetry. In the rhombohedral phase, due to the symmetry

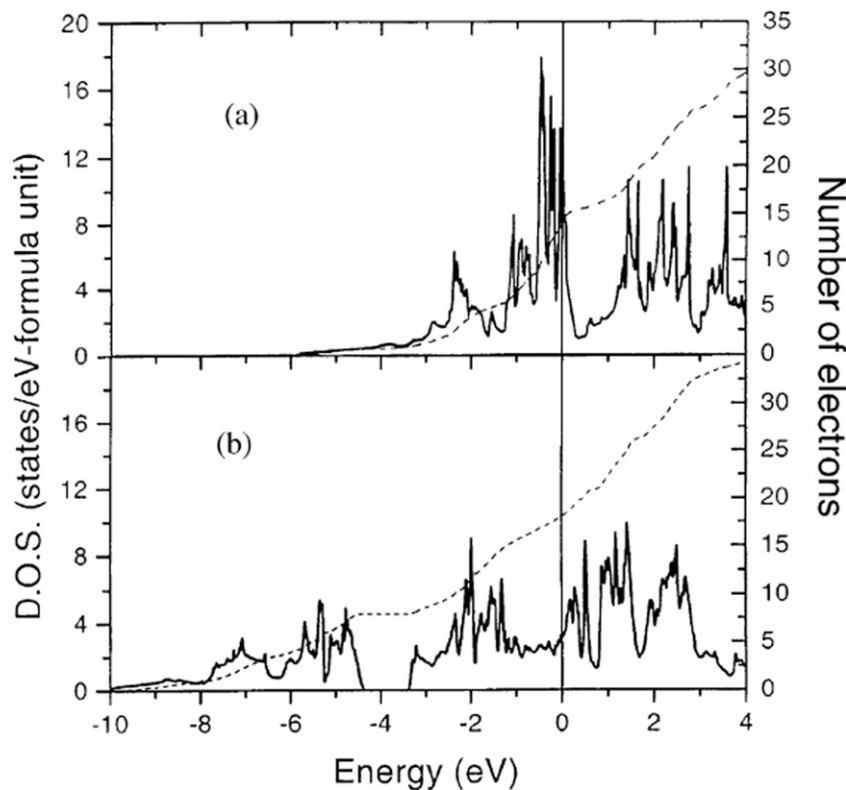


Fig. 6 Total density of states: solid line, left-hand-side scale; number of electrons, dashed line, right-hand-side scale. (a) ZrV_2 C-15 cubic phase, (b) ZrV_2H_4 . The origin of energies is the Fermi energy.

lowering, the Van Hove singularities of the DOS are considerably smoothed. The total DOS at E_F is found to decrease by 35% from its value in the cubic phase, a result consistent with the sharp decrease of the magnetic susceptibility observed at T_m . It is interesting to point out in this connection that two distinct superconducting transitions differing by 1K have been observed experimentally by Däumer *et al.* [118] and it has been suggested that the two phases are superconducting, the higher T_c value being attributed to small amounts of untransformed cubic C-15 phase.

The DOS of ZrV_2H_4 calculated using the structural data of Didisheim *et al.* [119] in the low-temperature tetragonal phase in which the hydrogen atoms order at one of the Zr_2V_2 sites is plotted in Fig. 6. The metal–hydrogen bonding states form four bands per formula unit, extending from -10.3 and -4.4 eV below E_F . The hydrogen interaction with zirconium is slightly larger but of the same order of magnitude than that with the vanadium states. The DOS at E_F is 72% lower than in the pure intermetallic. In the hydride, as in the pure intermetallic, the states at E_F have mostly a vanadium d character. In contrast to the pure intermetallic, the vanadium p contribution at E_F is much smaller since the vanadium p states are rather found to participate in the metal–hydrogen low-energy states. The band width and structures obtained in the calculated DOS of ZrV_2 and ZrV_2H_4 are in good agreement with UV and X-ray photoemission data of Schlapbach *et al.* [120] and X-ray emission spectroscopic results.

The results of electronic structure calculations can be used in conjunction with experimental data on the vibrational properties to estimate the electron–phonon coupling constant l which essentially determines the value of T_c . Band structure calculations show that the electronic contribution of the electron–acoustic phonon coupling is drastically reduced from the intermetallic to the hydride due to a large decrease of the DOS at E_F and to a reduced value of the vanadium p orbital character of the electronic states. The electronic contribution of the electron–optical phonon is very small because the Fermi level of the hydride falls into the metal d bands unlike in superconducting PdH. For these two reasons, hydrogen absorption leads to the disappearance of the superconducting properties.

(b) Hydrides of magnetic Laves phases

A first-principles calculations of hexagonal C14-type Laves phase Ti–Mn metals and their hydrides, namely, $Ti_{1.0}Mn_{2.0}H_3$, $Ti_{1.25}Mn_{1.75}H_3$, and $Ti_{1.5}Mn_{1.5}H_3$ were performed, to understand their hydrogen storage properties, particularly focusing on materials trend of the heat of formation. The ultrasoft pseudopotential method within the generalized gradient approximation to density functional theory were employed. The effects of magnetic ordering was neglected and assumed that all hydrogen atoms are located on the 12 k sites of the space group P63/mmc. It has been found that the calculated heat of formation reproduces the experimental trend, and it involves two dominant contributions: (1) from an energy cost by volume expansion, and (2) from an energy gain by hydrogen insertion. Thus an equilibrium volume and a bulk modulus of the host metal are the keys to describe the heat of formation for these systems (see Ref. [121] for reviews).

The influence of hydrogen absorption on the magnetic properties of Laves phase AB₂ compounds, where A is a transition or rare earth element and B a magnetic or nonmagnetic transition element, is a very vast and fascinating topic that has been experimentally investigated since the pioneering work of Buschow *et al.* [122,123]. Due to the great complexity of the phase diagrams and crystal and magnetic structures observed, ab initio investigations of these hydrides remain scarce, particularly for systems involving 4f electrons of magnetic rare earths and 3d moments on the transition elements, which raise the controversy of the validity of localized versus band models.

The insertion of hydrogen in the matrix is expected to affect the magnetic properties via several factors: magnetism is strongly dependent on interatomic distances that increase by the negative pressure effect associated with hydrogen uptake; in addition, the metal hydrogen bonding and the change in the Fermi level position are expected to strongly modify the magnetic interactions between A and B atoms. We shall discuss here band structure results only on magnetic cubic (C-15) AB₂ compounds (A=Y, B=Mn, Fe) and their hydrides.

YMn_2 is found to be an antiferromagnet: the moments obtained in spin-polarized LMTO calculations, 2.6 mB per manganese atom, are in satisfactory agreement with the experimental value of 2.7 mB found by Nakamura *et al.* [124] and previous LMTO [125] and tight-binding Hartree-Fock calculations. The total energy of the antiferromagnetic state is 8 mRy lower than that of the paramagnetic phase and the calculated volume change at the antiferromagnetic–paramagnetic transition agrees with thermal expansion measurements. The hydrogen absorption has been investigated since the work of Buschow *et al.* [122]. The band structure of $YMnH_x$ at low ($x=0.521$) [125] and high ($x=4$) hydrogen concentrations has been investigated. Total energies performed for three different hydrogen positions in the low concentration limit favor the tetrahedral A2B2 sites, as observed experimentally. The hydrogenated compounds are found to be antiferromagnetic with a small ferrimagnetic component. At all hydrogen concentrations, the volume expansion leads to an increase of the magnetic moments while the Mn–H bonding interaction tends to decrease the magnetic moment. The change in the magnetic properties as a function of hydrogen concentration is rather complex (see Refs. [126] and [127]) and has not yet been fully studied theoretically. The magnetic properties of YFe_2 obtained from band structure calculations show, in agreement with experimental data of Buschow and van Diepen [122] and later work, that the intermetallic is ferromagnetic, with a calculated total magnetic moment of 2.86 mB compared to the experimental value of 2.9 mB. The moment is essentially localized on the iron atoms; however a small ferrimagnetic contribution due to the more delocalized 4d orbitals appears on the yttrium sites. Two hydrides YFe_2H_x have been investigated assuming a hydrogen ordering ($x=3$) by an augmented spherical wave calculation (Ref. [128] and references therein) and by the LMTO method for $x=4$. For YFe_2H_4 it is found that the 20% lattice expansion leads to an increase of the moment up to 3.93 mB while the chemical metal–hydrogen interaction reduces this value as also observed for YFe_2H_3 and YMn_2H_x .

4 Hydrides of Intermetallic Compounds With Transition and Alkali or Alkaline-Earth Elements

The search for new storage materials of light weight and good hydrogen absorption capacities, as well as the fundamental interest in hydrides of metals with unusual coordination number or valence, led to the synthesis and characterization of a number of ternary hydrides of general composition $A_xM_yH_z$ where A forms binary insulating hydrides and B forms rather metallic hydrides (see Ref. [129] for reviews). These hydrides present interesting features from a theoretical point of view due to (1) the possible coexistence of ionic, covalent, and metallic bonding of hydrogen with A and B, (2) the electrical properties can vary from those of ionic insulators to metallic systems, and (3) the possibility of finding superconductivity.

4.1 Hydrides of the RNi_3 - and R_2Ni_7 -based (R =Light Rare Earth Element)

intermetallics exhibit novel structural features. Structures of these hydrides, including $CeNi_3D_{2.8}$, $La_2Ni_7D_{6.5}$, $LaNi_3D_{2.8}$, and $Ce_2Ni_7D_{4.7}$, were formed via a huge volume expansion occurring along a single crystallographic direction. Unique structural features during the formation of the hydrides include: (1) The lattice expansion proceeds exclusively within the RNi_2 slabs leaving the RNi_5 slabs unmodified. Such expansion, $\sim 60\%$ along $[0\ 0\ 1]$ for the Laves layers, is associated with occupation of these slabs by D atoms; (2) New types of interstitial sites occupied by D were formed; (3) An ordered hydrogen sublattice was observed. In the present work we give (1) a review of the crystal chemistry of the conventional, interstitial type hydrides formed by RT_3 and R_2T_7 intermetallic compounds (R =rare earths; T =Fe, Co, Ni) as compared to the unusual features of the crystal chemistry of anisotropic hydrides formed by the RNi_3 and R_2Ni_7 intermetallics and (2) studies of the interrelation between structure and bonding in anisotropic hydrides by performing density functional calculations for $CeNi_3$ and Ce_2Ni_7 intermetallic alloys and their corresponding hydrides. These studies provide an understanding of the bonding mechanism in the hydrogenated compounds which causes a complete anisotropic rebuilding of their structures. From DOS analysis, both initial intermetallics and their related hydrides were found to be metallic. Bader topological analysis for the non-hydrogenated intermetallics showed that Ce atoms donate in average of almost 1.2 electrons to the Ni sites. Hydrogenation increases electron transfer from Ce; its atoms donate 1.2–1.6 electrons to Ni and H. The Charge Density Distribution and Electron Localization Function for the $Ce_2Ni_7D_{4.7}$ phase clearly confirm that the interaction between the Ce and Ni does not have any significant covalent bonding. Ni is bonded with H via forming spatial frameworks $-H-Ni-H-Ni-$ where H atoms accumulate an excess electron density of $\sim 0.5e^-$. Thus, the tetrahedral or open saddle-type NiH_4 coordination observed in the structures of these hydrides is not associated with the formation of $[Ni^0H_4^{1-}]^{4-}$ complexes containing a hydrido-ion H^{-1} . In the structural frameworks there are terminal bonds Ni–H, bridges Ni–H–Ni, and the bonds where one H is bound to three different Ni. These spatial ordered frameworks stand as the principal reason for the anisotropic changes in the structural parameters on hydrogenation. Another unique feature of anisotropic hydrides is the donation of electrons from nonhydrogenated RNi_5 parts to hydrogen in RNi_2 slabs stabilising these fragments (see Ref. [130] for reviews).

4.2 Mg_2NiH_4 , Mg_2CoH_5 , Mg_2FeH_6 and Related Hydrides

Hydrides of the series A_2MH_6 (A =Mg, Ca, Sr, M =Fe, Ru, Os) crystallize in the cubic K_2PtCl_6 structure while Mg_2CoH_5 and Mg_2NiH_4 are present above 500K as a high-temperature cubic phase and low-temperature phases of lower symmetry. In the cubic phases the metal lattice is of antifluorite type with large M–M distances. The hydrogen atoms form octahedral cages around the M atom in A_2MH_6 with short M–H distances. The hydrogen positions of the high-temperature phases of Mg_2NiH_4 and Mg_2CoH_5 are believed to result from the thermal average of square planar or tetrahedral configurations around nickel and square pyramidal arrangement of hydrogen atoms around cobalt. These hydrides correspond to 18 valence electron compounds; the hydrogen content can be increased by a corresponding decrease of the transition metal valence.

The band structures can be interpreted in terms of coordination chemistry since the M–H cages are weakly coupled [69,131]. Two types of bonds coexist due to the covalent M–H interactions and the ionic character of the A element. The compounds are found to be insulating. In hydrides with octahedral coordination, A_2MH_6 , the gap opens between the three $M\ d-t_{2g}$ nonbonding and the $M\ d-eg$, hydrogen s antibonding states. In Mg_2NiH_4 , with tetrahedral NiH_4 cages, the gap occurs between the five nickel d nonbonding and the $Ni-H\ s$ antibonding states. In Mg_2CoH_5 with the square pyramidal configuration, the gap appears between the four nonbonding $M\ d$ and the antibonding dx^2y^2 hydrogen s antibonding states as expected from coordination chemistry. The maximum hydrogen content in these hydrides corresponds to the complete filling of bonding M–H and nonbonding M states, a situation that is known to be energetically favorable. The values of the energy gaps obtained in the LDA calculations are in reasonable agreement with experimental observations although they are expected to be affected by correlation effects in systems with narrow d bands.

4.3 Palladium-Based Ternary Hydrides

The first fully structurally characterized ternary europium palladium hydrides (deuterides) are reported by Kohlmann *et al.* [132]. The most Eu rich compound is Eu_2PdD_4 . Its β - K_2SO_4 type structure (space group $Pnma$, $a=749.47(1)$ pm, $b=543.34(1)$ pm, $c=947.91(1)$ pm, $Z=4$) contains tetrahedral 18-electron $[PdD_4]^{4-}$ complex anions and divalent Eu cations. The compound is

presumably nonmetallic and shows paramagnetic behavior (μ_{eff} 8.0(2) (μ_{B}) with ferromagnetic ordering at $T_{\text{C}}=15.1(4)\text{K}$. A metallic compound at intermediate Eu content is EuPdD_3 . It crystallizes with the cubic perovskite structure (space group $\text{Pm}\bar{3}\text{m}$, $a=380.01(2)$ pm, $Z=1$) in which palladium is octahedrally surrounded by fully occupied deuterium sites. Metallic hydrides at low Eu content form by reversible hydrogen absorption of intermetallic EuPd_2 (Fd_3hm , $a=775.91(1)$ pm, $Z=8$). Depending on the experimental conditions at least three phases with distinctly different hydrogen contents x exist: $\text{EuPd}_2\text{H}_{x\approx 0.1}$ ($a=777.02(2)$ pm, $Z=8$, $T=298\text{K}$, $p(\text{H}_2)=590$ kPa), $\text{EuPd}_2\text{H}_{x\approx 0.15}$ ($a=794.47(5)$ pm, $Z=8$, $T=298\text{K}$, $p(\text{H}_2)=590$ kPa), and $\text{EuPd}_2\text{H}_{x\approx 2.1}$ ($a=802.1(1)$ pm, $Z=8$, $T=350\text{K}$, $p(\text{H}_2)=610$ kPa). All crystallize with cubic Laves phase derivative structures and have presumably disordered hydrogen distributions (see Ref. [133] for review).

Since hydrides of palladium and its alloys with filled d bands are superconductors with moderate but sizeable critical temperatures (PdH ($T_{\text{C}}=9\text{K}$), $\text{Pd}_{0.55}\text{Cu}_{0.45}\text{H}_{0.7}$ ($T_{\text{C}}=16\text{K}$)), the synthesis of ternary hydrides of palladium with filled d bands and electronic properties at the Fermi level similar to those of PdH could result in an important electron optical phonon coupling and superconductivity. Li_2PdH_2 and Na_2PdH_2 have been synthesized by Kadir *et al.* [134]. These hydrides are characterized by a body-centered tetragonal array of linear PdH_2 entities along the c -axis of the tetragonal unit cell, with short Pd–H distances. According to conventional valencies these compounds should be insulating; however, band structure calculations by Gupta [132] and Switendick [135] show that these 14 valence electron hydrides are rather semimetallic with a low DOS at E_{F} associated to a weak overlap between the seven palladium d, hydrogen s derived bands and the eighth band mostly due to lithium or sodium p states. The crystal structure of K_2PdH_4 is characterized by a b.c.t. array of square planar PdH_4 units with short Pd–H distances; this 16 valence electron hydride is found to be insulating with a gap of 1.8 eV. Its electronic structure can be interpreted in terms of coordination chemistry of $(\text{PdH}_4)^{-4}$ entities, with square planar $\text{D}_{4\text{h}}$ point group, interacting only weakly, the alkali counterion neutralizing the structure.

Platinum-based compounds such as K_2PtH_4 and Na_2PtH_4 have also been synthesized and characterized. In these hydrides, the PtH_4 units have different orientations than in the palladium-based compounds. These quasimolecular complexes are all found to be insulating [137]. The electronic structure of the palladium-based cubic perovskite structure APdH_3 ($A=\text{Sr}, \text{Eu}, \text{Yb}$) and the complex hydride $\text{PdSr}_2\text{LiH}_5$ has been investigated in connection with the possible occurrence of superconductivity. In the hydrides APdH_3 the electrons of the divalent element are essentially transferred to the Pd–H states, the main part of the d bands of palladium are essentially filled, and the Fermi level falls in the antibonding Pd–H states. These hydrides are metallic with DOSs at E_{F} as in PdH and noble metals. The crystal structure of the complex $\text{PdSr}_2\text{LiH}_5$ hydride can be understood from the stacking of cubic perovskite insulating SrLiH_3 subunits and defective perovskite SrPdH_2 . A metallic behavior is found for $\text{PdSr}_2\text{LiH}_5$. As in APdH_3 , the essential part of the palladium d states are filled and a non-negligible contribution of the hydrogen s states is found at E_{F} . A study of the electronic part of the electron–phonon coupling shows that the hydrogen contribution is non-negligible, although it is always smaller than in superconducting PdH . If the optical phonon modes, not yet known, are not too high, hydrides of this family could be potential candidates for superconductivity. Experimentally only NaPd_3H_2 , which can be viewed as a distorted sodium-substituted palladium hydride, has been found to be superconducting below 2K, while CaPd_3H is metallic but not superconducting as shown by Rönnebro *et al.* [136].

5 Perspective

Band structure calculations have greatly improved, at a microscopic level, our understanding of the electronic properties of metal–hydrogen systems. In the near future, further progress needs to be made in the study of compounds of greater structural complexity, in the areas of the thermodynamic and elastic properties, and especially in the rich field of magnetism.

Acknowledgments

Reshak would like to acknowledge the CENTEM project, reg. no. CZ.1.05/2.1.00/03.0088, cofunded by the ERDF as part of the Ministry of Education, Youth and Sports OP RDI programme and, in the follow-up sustainability stage, supported through CENTEM PLUS (LO1402) by financial means from the Ministry of Education, Youth and Sports under the National Sustainability Programme I. Computational resources were provided by MetaCentrum (LM2010005) and CERIT-SC (CZ.1.05/3.2.00/08.0144) infrastructures.

References

- [1] Schlapbach, L., Züttel, A., 2001. Hydrogen-storage materials for mobile applications. *Nature* 414, 353–358.
- [2] Züttel, A., 2003. Materials for hydrogen storage. *Mater. Today* 6, 24–33.
- [3] Bobet, J.-L., Even, C., Nakamura, Y., Akiba, E., Darriet, B., 2000. Synthesis of magnesium and titanium hydride via reactive mechanical alloying. Influence of 3D-metal addition on MgH_2 synthesis. *J. Alloys Compd.* 298, 279–284.
- [4] Liang, G., Huot, J., van Neste, A., Schulz, R., 1999. Catalytic effect of transition metals on hydrogen sorption in nanocrystalline ball milled MgH_2 – Tm ($\text{Tm}=\text{Ti}, \text{V}, \text{Mn}, \text{Fe}$ and Ni) systems. *J. Alloys Compd.* 292, 247–252.
- [5] Jain, I.P., Lal, Ch., Jain, A., 2010. Hydrogen storage in Mg: A most promising material. *Int. J. Hydrogen Energy* 35, 5133–5144.

- [6] Liang, G., Schulz, R., 2003. Synthesis of Mg–Ti alloy by mechanical alloying. *J. Mater. Sci.* 38, 1179–1184.
- [7] Zaluski, L., Zaluska, A., Strom-Olsen, J.O., 1997. Nanocrystalline metal hydrides. *J. Alloys Compd.* 253–254, 70–79.
- [8] Bassetti, A., Bonetti, E., Pasquini, L., *et al.*, 2005. Hydrogen desorption from ball milled MgH₂ catalyzed with Fe. *Eur. Phys. J. B* 43, 19–27.
- [9] Gupta, R.B., 2009. Hydrogen fuel production transport and storage, first ed. Boca Raton, FL: CRC Press.
- [10] Varin, R.A., Czujko, T., Wronski, Z.S., 2009. Nanomaterials for solid state hydrogen storage, first ed. New York, NY: Springer Science Bussines Media.
- [11] Hirscher, M., 2010. Handbook of hydrogen storage: New materials for future energy storage, first ed. Weinheim: Wiley-VCH Verlag GmbH & Co. KgaA.
- [12] Walker, G., 2008. Solid-state hydrogen storage, Materials and Chemistry, first ed. Cambridge: Woodhead Publishing Limited.
- [13] Fukai, Y., 2005. The metal–hydrogen system, second ed. Berlin: Springer.
- [14] Borgschulte, A., Schlapbach, L., 2008. In: Zuttel, A. (Ed.), Hydrogen as A Future Energy Carrier, first ed. Weinheim: Wiley-VCH Verlag GmbH & Co. KgaA.
- [15] Bowman, R.C., 1971. Cohesive energies of the alkali hydrides and deuterides. *J. Phys. Chem.* 75, 1251–1255.
- [16] Luaña, V., Pueyo, L., 1990. Simulation of ionic crystals: The ab initio perturbed-ion method and application to alkali hydrides and halides. *Phys. Rev. B* 41, 3800–3814.
- [17] Wolverton, C., Ozoliņš, V., Asta, M., 2004. Hydrogen in aluminum: First-principles calculations of structure and thermodynamics. *Phys. Rev. B* 69, 144109:1–144109:16.
- [18] Vidal-Valat, G., Vidal, J.P., Kurki-Suonio, K., Kurki-Suonio, R., 1992. Evidence on the breakdown of the Born–Oppenheimer approximation in the charge density of crystalline 7LiH/D. *Acta Cryst. A* 48, 46–60.
- [19] Blat, D.K., Zein, N.E., Zinenko, V.I., 1991. Calculations of phonon frequencies and dielectric constants of alkali hydrides via the density functional method. *J. Phys. Condens. Matter* 3, 5515–5524.
- [20] Ivanović, N., Novaković, N., Colognesi, D., Radisavljević, I., Ostojić, S., 2010. Electronic principles of some trends in properties of metallic hydrides. *Int. J. Mod. Phys. B* 24, 703–710.
- [21] Smithson, H., Marianetti, C.A., Morgan, D., *et al.*, 2002. First-principles study of the stability and electronic structure of metal hydrides. *Phys. Rev. B* 66, 144107:1–144107:10.
- [22] Lebegue, S., Alouani, M., Arnau, B., Pickett, W.E., 2003. Pressure-induced simultaneous metal–insulator and structural-phase transitions in LiH: A quasiparticle study. *Europhys. Lett.* 63, 562–568.
- [23] Novaković, N., Radisavljević, I., Colognesi, D., Ostojić, S., Ivanović, N., 2007. First principle calculations of alkali hydride electronic structures. *J. Phys. Condens. Matter* 19, 406211:1–406211:14.
- [24] Vajeeston, P., 2004 Theoretical modeling of hydrides. PhD Thesis, University of Oslo, Oslo, Norway.
- [25] Ravindran, P., Vajeeston, P., Fjellvåg, H., Kjekshus, A., 2004. Chemical-bonding and high-pressure studies on hydrogen-storage materials. *Comput. Mater. Sci.* 30, 349–357.
- [26] Ceriotti, M., Miceli, G., Pietropaolo, A., *et al.*, 2010. Nuclear quantum effects in ab initio dynamics: Theory and experiments for lithium imide. *Phys. Rev. B* 82, 174306:1–174306:5.
- [27] Bogdanović, B., Schwickardi, M., 1997. Ti-doped alkali metal aluminium hydrides as potential novel reversible hydrogen storage materials. *J. Alloys Compd.* 253–254, 1–9.
- [28] Bogdanović, B., Brand, R.A., Marjanović, A., Schwickardi, M., Tölle, J., 2000. Metal-doped sodium aluminium hydrides as potential new hydrogen storage materials. *J. Alloys Compd.* 302, 36–58.
- [29] Vajeeston, P., Ravindran, P., Vidya, R., Fjellvåg, H., Kjekshus, A., 2003. Pressure-induced phase of NaAlH₄: A potential candidate for hydrogen storage? *Appl. Phys. Lett.* 82, 2257–2259.
- [30] Chen, P., Xiong, Z., Luo, J., Lin, J., Tan, K.L., 2002. Interaction of hydrogen with metal nitrides and imides. *Nature* 420, 302–304.
- [31] Luo, W., Rönnebro, E., 2005. Towards a viable hydrogen storage system for transportation application. *J. Alloys Compd.* 404–406, 392–395.
- [32] Ivanović, N., Radisavljević, I., Novaković, N., Manasijević, M., Colognesi, D., 2011. Calculations of molecular structures and processes important for hydrogen behaviour in the Li–amide/imide system. *Acta Phys. Pol.* 119, 242–245.
- [33] Dyck, W., Jex, H., 1981. Lattice dynamics of alkali hydrides and deuterides with the NaCl type structure. *J. Phys. C Solid State Phys.* 14, 4193–4215.
- [34] Yu, R., Lam, P.K., 1988. Electronic and structural properties of MgH₂. *Phys. Rev. B* 37, 8730–8737.
- [35] Kunz, A.B., Mickish, D.J., 1975. Electronic structure of LiH and NaH. *Phys. Rev. B* 11, 1700–1704.
- [36] Grosso, G., Parravicini, G.P., 1979. Hartree-Fock energy bands by the orthogonalized-plane-wave method: Lithium hydride results. *Phys. Rev. B* 20, 2366–2372.
- [37] Zeng, K., Klassen, T., Oelerich, W., Bormann, R., 1999. Critical assessment and thermodynamic modeling of the Mg–H system. *Int. J. Hydrogen Energy* 24, 989–1004.
- [38] Miademma, A.R., 1973. The electronegativity parameter for transition metals: Heat of formation and charge transfer in alloys. *J. Less Common Met.* 32, 117–136.
- [39] Reshak, A.H., 2013. MgH₂ and LiH metal hydrides crystals as novel hydrogen storage material: Electronic structure and optical properties. *International Journal of Hydrogen Energy* 38 (2013), 1194–11954.
- [40] Ivanović, N., Novaković, N., Radisavljević, I., Matović, L., Novaković, J.G., 2012. Electronic principles of hydrogen incorporation and dynamics in metal hydrides. *Crystals* 2, 1261–1282. doi:10.3390/cryst2031261.
- [41] Reshak, A.H., Shalaginov, M.Y., Saeed, Y., Kityk, I.V., Auluck, S., 2011. First-principles calculations of structural, elastic, electronic, and optical properties of perovskite-type KMgH₃ crystals: Novel hydrogen storage material. *J. Phys. Chem. B* 115, 2836–2841.
- [42] Park, H.-H., Pezat, M., Darriet, B., Hagenmuller, P., 1987. *J. Less-Common Met.* 136, 1.
- [43] Vajeeston, P., Ravindran, P., Kjekshus, A., Fjellvåg, H., 2008. First-principles investigations of the MMgH₃ (M=Li, Na, K, Rb, Cs) series. *J. Alloys Compd.* 450, 327.
- [44] Klaveness, A., Swang, O., Fjellvåg, H., 2006. Formation enthalpies of NaMgH₃ and KMgH₃: A computational study. *Europhys. Lett.* 76, 285.
- [45] Schumacher, R., Weiss, A.J., 1990. KMgH₃ single crystals by synthesis from the elements. *Less-Common Met.* 163, 179–183.
- [46] Karazhanov, S.Zh., Ulyashin, A.G., Ravindran, P., Vajeeston, P., 2008. Semiconducting hydrides. *EPL* 82, 17006.
- [47] Vajeeston, P., Ravindran, P., Kjekshus, A., Fjellvåg, H., 2008. First-principles investigations of the MMgH₃ (M=Li, Na, K, Rb, Cs) series. *J. Alloys Compd.* 450, 327.
- [48] Yvon, K., King, R.B. (Eds.), 1994. *Encyclopedia of Inorganic Chemistry*, vol. 3. New York: Wiley.
- [49] Mamatha, A., Bogdanovic, B., Felderhoff, M., *et al.*, 2006. Mechanochemical preparation and investigation of properties of magnesium, calcium and lithium–magnesium alanates. *J. Alloys Compd.* 407, 78.
- [50] Ghebouli, B., Ghebouli, M.A., Fatmi, M., 2010. First-principles study of the structural, elastic, electronic, optical and thermodynamic properties of the perovskite XLiH₃ (X=Ba and Sr) under high pressure. *Eur. Phys. J. Appl. Phys.* 51, 20302.
- [51] Ghebouli, B., Ghebouli, M.A., Fatmi, M., 2010. First-principles study of structural, elastic, electronic and optical properties of perovskites XCaH₃ (X=Cs and Rb) under pressure. *Solid State Sci* 12, 587–596.
- [52] van Vucht, J.H.N., *et al.*, 1970. Philips Res. Rep. 25, 133. [SD-008]. 6.
- [53] Mueller, W.M., Blackledge, J.P., Libowitz, G.G., 1968. *Metal Hydrides*. New York: Academic Press.
- [54] Alefeld, G., Völkl, J., 1978. Hydrogen in Metals I and II, Topics in Applied Physics, vols. 28 and 29. Heidelberg: Springer.
- [55] Buschow, K.H.J., Bouten, P.C., Miedema, A.R., 1982. Hydrides formed from intermetallic compounds of two transition metals. *Rep. Prog. Phys.* 45, 937–1039.
- [56] Schlapbach, L. (Ed.), 1988. Hydrogen in Intermetallic Compounds I, Topics in Applied Physics, vol. 63. Heidelberg: Springer.
- [57] Schlapbach, L. (Ed.), 1992. Hydrogen in Intermetallic Compounds II, Topics in Applied Physics, vol. 67. Heidelberg: Springer.
- [58] Fukai, Y., 1992. *The Metal Hydrogen System*, Springer Series in Materials Science, vol. 21. Heidelberg: Springer.
- [59] Wipf, H., 1997. Hydrogen in Metals III, Topics in Applied Physics, vol. 73. Berlin: Springer.
- [60] Hohenberg, P., Kohn, W., 1964. Inhomogeneous electron gas. *Phys. Rev.* 136, B864–B871.

- [61] Skriver, H.L., 1983. The LMTO Method, Springer Series in Solid State Sciences, vol. 417. Berlin: Springer.
- [62] Singh, D.J., 1994. Plane Waves, Pseudopotentials, and the LAPW Method. Boston: Kluwer.
- [63] Dufek, P., Blaha, P., Schwarz, K., 1994. Phys. Rev. B 50, 7279.
- [64] Engel, E., Vosko, S.H., 1993. Phys. Rev. B 47, 13164.
- [65] Mokhtari, A., Akbarzadeh, H., 2003. Physica B 337, 122.
- [66] Tran, F., Blaha, P., 2009. Accurate band gaps of semiconductors and insulators with a semilocal exchange-correlation potential. Phys. Rev. Lett. 102, 226401.
- [67] Nicholson, K.M., Sholl, D.S., 2014. First-principles screening of complex transition metal hydrides for high temperature applications. Inorg. Chem. 53 (22), 11833–11848.
- [68] Switendick, A., 1978. The change in electronic properties on hydrogen alloying and hydride formation. In: Alefeld, G., Völkl, J. (Eds.), Hydrogen in Metals I, Topics in Applied Physics, vol. 28. Heidelberg: Springer, pp. 101–129. (Chapter 5).
- [69] Gupta, M., Schlapbach, L., 1988. Electronic properties. In: Schlapbach, L. (Ed.), Hydrogen in Intermetallic Compounds I, Topics in Applied Physics, vol. 63. Heidelberg: Springer, pp. 139–209. (Chapter 5).
- [70] Jena, P., Satterthwaite, C.B., 1983. Electronic Structure and Properties of Hydrogen in Metals, NATO ASI Series, vol. 6. New York: Plenum.
- [71] Vajda, P., 1995. Hydrogen in rare-earth metals including RH₂px phases. In: Gschneidner, K.A. (Ed.), Handbook on the Physics and Chemistry of Rare Earths, vol. 20. Amsterdam: North Holland, p. 207.
- [72] Huijberts, J.N., Griessen, R., Rector, J.H., *et al.*, 1996. Yttrium and lanthanum hydride films with switchable optical properties. Nature (London) 380, 231–234.
- [73] Yan, W., Chou, M.Y., 1995. Structural and electronic properties of hexagonal yttrium trihydride. Phys. Rev. B 51, 7500–7507.
- [74] Eder, S.J., Pen, H.F., Sawatzki, G.A., 1997. Kondo-lattice-like effects of hydrogen in transition metals. Phys. Rev. B 56, 10115–10120.
- [75] Van der Molen, S.J., Welling, M.S., Griessen, R., 2000. Correlated electromigration of H in the switchable mirror YH₃-d. Phys. Rev. Lett. 85, 3882–3885.
- [76] Ng, K.K., Zhang, F.C., Anisimov, V.I., Rice, T.M., 1999. Theory for metal hydrides with switchable optical properties. Phys. Rev. B 59, 5398–5413.
- [77] Kelly, P.J., Dekker, J.P., Stumpf, R., 1997. Theoretical prediction of the structure of insulating YH₃. Phys. Rev. Lett. 78, 1315–1318.
- [78] Udovic, T.J., Rush, J.J., Huang, Q., Rush, J.J., Anderson, I.S., 1997. Neutron scattering studies of the structure and dynamics of rare-earth hydrides and deuterides. J. Alloys Compd. 253–4, 241–247.
- [79] van Gelderen, P., Bobbert, P.A., Kelly, P.J., Brocks, G., 2000. Parameter-free quasiparticle calculations for YH₃. Phys. Rev. Lett. 85, 2989–2992.
- [80] Miyake, T., Aryasetiawan, F., Kino, H., Terakura, K., 2000. GW quasiparticle band structure of YH₃. Phys. Rev. B 61, 16491–16496.
- [81] van Gelderen, P., Kelly, P.J., Brocks, G., 2001. Phonon spectrum of YH₃: Evidence for a broken symmetry structure. Phys. Rev. B 63, 100301.
- [82] Zogal, X., Nimtz, M., Rohde, M., Bokranz, W., Römmling, U., 2001. The multicellular morphotypes of *Salmonella typhimurium* and *Escherichia coli* produce cellulose as the second component of the extracellular matrix. Mol. Microbiol. 39, 1452–1463.
- [83] Wang, Y., Chou, M.Y., 1994. Pseudopotential plane-wave study of a-YHx. Phys. Rev. B 49, 13357–13365.
- [84] Tarasov, B.P., Fokin, V.N., Fokin, E.E., Yartys, V.A., 2015. Synthesis of hydrides by interaction of intermetallic compounds with ammonia. J. Alloys Compd. <http://dx.doi.org/10.1016/j.jallcom.2015.01.007>
- [85] Libowitz, G.G., Hayes, H.F., Gibb Jr., T.R.P., 1958. The system zirconium–nickel and hydrogen. J. Phys. Chem. 62, 76–79.
- [86] Dantzer, P., 1997. Metal–hydride technology: A critical review. In: Wipf, H. (Ed.), Hydrogen in Metals III, Topics in Applied Physics, vol. 73. Berlin: Springer, pp. 279–331. (Chapter 7).
- [87] Reilly, J.J., Wiswall, R.H., 1974. Formation and properties of iron titanium hydride. Inorg. Chem. 13, 218.
- [88] Hilscher, G., Wiesinger, G., 1991. Magnetism of hydrides. In: Buschow, K.H.J. (Ed.), Magnetic Materials, vol. 6. Amsterdam: North Holland.
- [89] Penzhorn, R.D., Devillers, M., Sirch, M., *et al.*, 1995. Hydrogen sorption rate by intermetallic compounds suitable for tritium storage. Fusion Technol. 28, 1437.
- [90] Shmayda, W.T., Heics, A.G., Kherani, N.P., 1990. Comparison of uranium and zirconium cobalt for tritium storage. J. Less-Common Met. 162, 117–127.
- [91] Longhurst, G.R., 1988. Pyrophoricity of tritium-storage bed materials. Fusion Technol. 14, 750.
- [92] Tan, G.L., Liu, X.P., Jiang, L.J., *et al.*, 2007. Dehydrogenation characteristic of Zr_{1-x}MxCo (M=Hf,Sc) alloy. Trans. Nonferrous Met. Soc. China 17, 949–953.
- [93] Meleg, T., Deaconu, M., Ducu, C., Dinu, A., 2009. Zr–Co hydrides stability against heating-cooling cycles in a closed system. J. Mater. Sci. Eng. 3, 61.
- [94] Gupta, M., 1999. Electronic structure and stability of hydrides of intermetallic compounds. J. Alloys Compd. 293–295, 190–201.
- [95] Westlake, D.G., Shaked, H., Mason, P.R., McCart, B.R., Muller, M.H., 1982. Interstitial site occupation in ZrNiH. J. Less-Common Met. 88, 17–23.
- [96] Koroteev, Y.M., Lipnitskii, A.G., Chulkov, E.V., Silkin, V.M., 2002. The (110) surface electronic of FeTi, CoTi, and NiTi. Surf. Sci. 507, 199–206.
- [97] Verdineili, V., German, E., Jasen, P., Gonzalez, E., Marchetti, J.M., 2014. The influence of pre-adsorbed Pt on hydrogen adsorption on B2 FeTi(111). Int. J. Hydrogen Energy 39, 8621e30.
- [98] Reilly, J.J., Wiswall, R.H., 1974. Formation and properties of iron titanium hydride. Inorg. Chem. 13 (1), 218e22.
- [99] Wipf, H. (Ed.), 1995. Hydrogen in Metals III, Topics in Applied Physics, vol. 73. Springer-Verlag.
- [100] Takeshita, T., Gschneidner Jr., K.A., Lakner, J.F., 1981. J. Less-Common Met. 78, 43.
- [101] Percheron-Guegan, A., Grandjean, F., 1995. Interstitial intermetallic alloys. In: Long, G.J., Buschow, K.H.J. (Eds.), NATO ASI Series: Applied Sciences, vol. 281. Kluwer Academic Publisher, p. 77.
- [102] Takeshita, T., Gschneidner Jr., K.A., Thome, D.K., McMasters, O.D., 1980. Phys. Rev. B 21, 5636.
- [103] Chung, Y., Takeshita, T., McMasters, O.D., Gschneidner Jr., K.A., 1980. J. Less-Common Met. 74, 217.
- [104] Leisure, R.G., Foster, K., Hightower, J.E., Ode, A., Skripov, A.V., 2002. J. Alloys Compd. 330–332, 396.
- [105] Berezniisky, M., Ode, A., Hightower, J.E., Yeheskel, O., Jacob, I., Leisure, R.G., 2002. J. Appl. Phys. 91, 5010.
- [106] Yeheskel, O., Natrass, C.E., Leisure, R.G., Jacob, I., Bowman Jr., R.C., 2004. J. Appl. Phys. 95, 1089.
- [107] Hector Jr., L.G., Herbst, J.F., Capehart, T.W., 2003. J. Alloys Compd. 353, 74.
- [108] Crivello, J.C., Gupta, M., 2005. Relationship between compressibility and hydrogen absorption in some Haucke compounds. J. Alloys Compd. 404–406, 565–569.
- [109] Gupta, M., 1998. Effect of substitutions at the nickel site on the electronic structure of LaNi₅ and its hydrides. In: Nickel, N.H., Jackson, W.B., Bowman, R.C., Leisure, R.G. (Eds.), MRS Symp. Proc., Symposium: H in Semiconductors and Metals, vol. 513. Warrendale, PA: Materials Research Society, pp. 79–84.
- [110] Nakamura, H., Nguyen-Manh, D., Pettifor, D., 1998. Electronic structure and energetics of LaNi₅, a-La₂Ni₁₀H and b-La₂Ni₁₀H₁₄. J. Alloys Compd. 281, 81–91.
- [111] Tatsumi, K., Tanaka, I., Inui, H., Tanaka, K., Yamaguchi, M., Adachi, H., 2001. Atomic structures and energetics of LaNi₅-H solid solution and hydrides. Phys. Rev. B 64, 184105.
- [112] Percheron-Guegan, A., 1995. A survey of binary and ternary metal hydride systems. In: Grandjean, F., Long, G.J., Buschow, H.K.J. (Eds.), Interstitial Intermetallic Compounds, NATO ASI Series, Vol. 281. Dordrecht: Kluwer, pp. 77–105. (Chapter 5).
- [113] Takeshita, T., Dublon, G., McMaster, O.D., Gschneidner, K.A., 1980. Low temperature heat capacity studies on hydrogen absorbing intermetallic compounds. In: McCarty, G.J., Rhyne, J.J., Silver, H.B. (Eds.), Rare Earths in Modern Science and Technology, vol. 2. New York: Plenum, p. 563.
- [114] Griessen, R., Riederer, T., 1988. Heats of formation models. In: Schlapbach, L. (Ed.), Hydrogen in Intermetallic Compounds I, Topics in Applied Physics, vol. 63. Heidelberg: Springer, pp. 221–284. (Chapter 6).
- [115] Yang, J.B., Tai, C.Y., Marasinghe, G.K., *et al.*, 2000. Structural, electronic, and magnetic properties of LaNi₅ xTx (T=4Fe, Mn) compounds. Phys. Rev. B 63, 014407.
- [116] Moncton, D.E., 1973. Lattice transformation in the superconductor ZrV₂ by neutron diffraction. Solid State Commun. 13, 1779–1782.
- [117] Klein, B.M., Pickett, W.E., Papaconstantopoulos, D.A., 1983. Electronic structure, superconductivity, and magnetism in the C-15 compounds ZrV₂, ZrFe₂, ZrCo₂. Phys. Rev. B 27, 6721–6731.

- [118] Daumer, W., Kahn, H.R., Kobler, U., Luders, C., 1989. Temperature dependent magnetic susceptibility and superconductivity of cubic Laves phase C-15 hydrides. *Phys. Lett. A* 138, 323–328.
- [119] Didisheim, J.J., Yvon, K., Fischer, P., Tissot, P., 1981. Order-disorder phase transition in $ZrV_2D_{3.6}$. *Solid State Commun.* 38, 637–641.
- [120] Schlapbach, L., Osterwalder, J., Riesterer, T., 1984. Recent experimental results on the electronic structure of binary and ternary hydrides. *J. Less-Common Met.* 103, 295–307.
- [121] Nagasako, Naoyuki, Fukumoto, Atsuo, Miwa, Kazutoshi, 2002. First-principles calculations of C14-type Laves phase Ti–Mn hydrides. *Phys. Rev. B* 66, 155106. (Published 14 October 2002; Erratum. *Phys. Rev. B* 66, 159902).
- [122] Buschow, K.H.J., van Diepen, A.M., 1976. Effect of hydrogen absorption on the magnetic properties of YFe_2 and $GdFe_2$. *Solid State Commun.* 19, 79–81.
- [123] Buschow, K.H.J., Sherwood, R.C., 1977. Magnetic properties and hydrogen absorption in rare-earth intermetallics of the type RMn_2 and R_6Mn_{23} . *J. Appl. Phys.* 48, 4643–4648.
- [124] Nakamura, H., Shiga, M., Kawano, S., 1983. Antiferromagnetism of YMn_2 intermetallic compound. *Physica B* 120, 212–215.
- [125] Pajda, M., Ahuja, R., Johansson, B., *et al.*, 1996. First-principles calculations of the magnetic properties of YMn_2 and its hydrides. *J. Phys. Condens. Matter* 8, 3373–3384.
- [126] Goncharenko, I.N., Mirebeau, I., Irodova, A.V., Suard, E., 1997. Interplay of magnetic and hydrogen orders in the Laves hydride $YMn_2H_{4.3}$. *Phys. Rev. B* 56, 2580–2584.
- [127] Latroche, M., Paul-Boncour, V., Percheron-Guegan, A., Bouree-Vigneron, F., Andre, G., 2000. Structural and magnetic properties of low D content YMn_2 deuteride. *J. Solid State Chem.* 154, 398–404.
- [128] Paul-Boncour, V., Percheron-Guegan, A., 1999. The influence of hydrogen on the magnetic properties and electronic structures of intermetallic compounds: YFe_2D_2 system as an example. *J. Alloys Compd.* 293–5, 237–242.
- [129] Yvon, K., 1994. Hydrides: Solid state transition metal complexes. In: King, R.B. (Ed.), *Encyclopedia of Inorganic Chemistry*. New York: Wiley, pp. 1401–1420.
- [130] Yartys, V.A., Vajeeston, P., Riabov, A.B., *et al.*, 2008. Crystal chemistry and metal-hydrogen bonding in anisotropic and interstitial hydrides of intermetallics of rare earth (R) and transition metals (T), RT3 and R2T7. *Z. Kristallogr.* 223, 674–689.
- [131] Garcia, G.N., Abriata, J.P., Sofo, J.O., 1999. Calculation of the electronic and structural properties of cubic Mg_2NiH_4 . *Phys. Rev. B* 59, 11746–11754.
- [132] Gupta, M., 1993. Electronic structure of hydrides containing alkali and alkaline-earth elements. *Z. Phys. Chem.* 181, 9–18.
- [133] Kohlmann, H., Fischer, H.E., Yvon, K., 2001. Europium palladium hydrides. *Inorg. Chem.* 40, 2608–2613.
- [134] Kadir, K., Kritikos, M., Noreus, D., Andresen, A.F., 1991. Metallic properties in the series $K_2Pd(II)H_4$, $Na_2Pd(0)H_2$ and $Li_2Pd(0)H_2$ correlated with the stabilization of a formally zero-valent palladium-hydrogen complex. *J. Less-Common Met.* 172–174, 36–41.
- [135] Switendick, A.C., 1993. The electronic structure of alkali metalnickel group-hydrogen compounds: Li_2PdH_2 and K_2PdH_4 . *Z. Phys. Chem.* 181, 19–25.
- [136] Rönnebro, E., Noréus, D., Kadir, K., Reiser, A., Bogdanovic, B., 2000. Investigation of the perovskite related structures of $NaMgH_3$, $NaMgF_3$ and Na_3AlH_6 . *J. Alloys Compd.* 299, 101–106.
- [137] Orgaz, E., Gupta, M., 2000. Chemical bonding features of the ternary alkali metal platinum and palladium hydrides. *Int. J. Quantum Chem.* 80, 141–152.

Further Reading

- Bronger, W., 1995. Synthesis and structure of new metal hydrides. *J. Alloys Compd.* 229, 1–9.
- Rao, B.K., Jena, P., 1985. Switendick criterion for stable hydrides. *Phys. Rev. B* 31, 6726–6730.